Optimality-based modelling of wheat sowing dates globally

Article

It is advisable to refer to the publisher's version if you intend to cite from the work. See Guidance on citing.

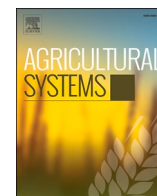# www.reading.ac.uk/centaur

CentAUR

Central Archive at the University of Reading

Optimality-based modelling of wheat sowing dates globally

Shengchao Qiao [a,b], Sandy P. Harrison [c,b], I. Colin Prentice [d,b], Han Wang [b,*]

[a] College of Ecology and Environment, Collaborative Innovation Center of Ecological Civilization, Hainan University, Haikou, China
[b] Department of Earth System Science, Ministry of Education Key Laboratory for Earth System Modeling, Institute for Global Change Studies, Tsinghua University, Beijing 100084, China
[c] School of Archaeology, Geography and Environmental Sciences (SAGES), University of Reading, Reading RG6 6AH, United Kingdom
[d] Georgina Mace Centre for the Living Planet, Department of Life Sciences, Imperial College London, Silwood Park Campus, Buckhurst Road, Ascot SL5 7PY, United Kingdom

HIGHLIGHTS

- Uncertainties in projected crop yields stem from specifying sowing dates; there is a need to predict sowing dates reliably.
- We investigate if wheat type and optimal sowing date can be predicted from climate constraints on phenology.
- Including constraints to avoid frost and rain damage in an optimality-based model gives good predictions of sowing dates.
- Global patterns in wheat type and sowing date, reflecting management practices to maximise local yields, are predictable.
- Our model can be used to predict climate change impacts on wheat yield and if changing sowing dates mitigate these impacts.

GRAPHICAL ABSTRACT
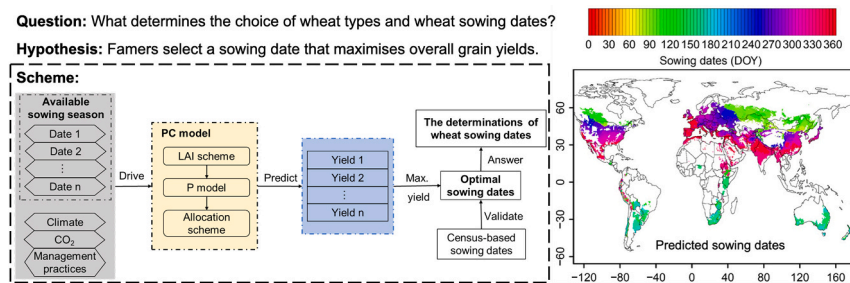
ABSTRACT

CONTEXT: Sowing dates are currently an essential input for crop models. However, in the future, the optimal sowing time will be affected by climate changes and human adaptations to these changes. A better understanding of what determines the choice of wheat type and sowing dates is required to be able to predict future crop yields reliably.
OBJECTIVE: This study was conducted to understand how climate conditions affect the choice of wheat types and sowing dates globally.
METHODS: We develop a model integrating optimality concepts for simulating gross primary production (GPP) with climate constraints on wheat phenology to predict sowing dates. We assume that wheat could be sown at any time with suitable climate conditions and farmers would select a sowing date that maximises yields. The model is run starting on every possible climatically suitable day, determined by climate constraints associated with low temperature and intense precipitation. The optimal sowing date is the day which gives the highest yield in each location. We evaluate the simulated optimal sowing dates with data on observed sowing dates created by

* Corresponding author.
  E-mail address: wang_han@mail.tsinghua.edu.cn (H. Wang).

merging census-based datasets and local agronomic information, then predict their changes under future climate scenarios to gain insight into the impacts of climate change.

RESULTS AND CONCLUSIONS: Cold-season temperatures are the major determinant of sowing dates in the extra-tropics, whereas the seasonal cycle of monsoon rainfall is important in the tropics. Our model captures the timing of reported sowing dates, with differences of less than one month over much of the world; maximum errors of up to two months occur in tropical regions with large altitudinal gradients. Discrepancies between predictions and observations are larger in tropical regions than temperate and cold regions. Slight warming is shown to promote earlier sowing in wet areas but later in dry areas; larger warming leads to delayed sowing in most regions. These predictions arise due to the interactions of several influences on yield, including the effects of warming on growing-season length, the need for sufficient moisture during key phenological stages, and the temperature threshold for vernalization of winter wheat.

SIGNIFICANCE: The integration of optimality concepts for simulating GPP with climate constraints on phenology provides realistic predictions of wheat type and sowing dates. The model thus provides a basis for predicting how crop calendars might change under future climate change. It can also be used to investigate potential changes in management to mitigate the negative impacts of climate change.

1. Introduction

Climate conditions affect the physiological processes of wheat (Jagadish et al., 2014). Temperature controls wheat phenology and thus the length of the required growing period (Wang et al., 2017a). Radiation affects the assimilation rate by determining energy supply (Wang et al., 2017b). Precipitation determines water availability for growth and transpiration (Elliott et al., 2014). All these processes contribute to determining wheat yield, which is therefore crucially dependent on climatic conditions during the growing period (Hernandez-Ochoa et al., 2018; Hunt et al., 2019; Ortiz-Bobea et al., 2021). Farmers generally decide whether winter or spring wheat is grown and select appropriate sowing dates to maximise yields on the basis of knowledge about the climate conditions in a given region (Waha et al., 2012).

Ongoing global warming is, however, already changing climate conditions in many wheat-growing areas and larger changes are expected in the future (Pörtner et al., 2022). Substantial reductions in wheat yields as a consequence of global warming are suggested by multiple lines of evidence, including field-warming experiments (Wang et al., 2020; Zhao et al., 2016), statistical regressions (Agnolucci et al., 2020; Schlenker and Roberts, 2019; Tack et al., 2015; Zhao et al., 2017) and crop modelling (Asseng et al., 2014; Zhao et al., 2017). Management changes, particularly changes in when wheat is sown, are likely to be necessary to offset the negative impacts of global warming on wheat production (Hunt et al., 2019). Indeed, there is already evidence that sowing dates have changed in response to recent climate changes (Lobell et al., 2013; Olesen et al., 2012).

Local agronomic knowledge and global data sets on sowing dates provide suitable information about the current situation (Kotsuki and Tanaka, 2015; Portmann et al., 2010; Sacks et al., 2010), but little guidance about the future adaptations that will be necessary with climate change. Process-based crop models could be used to project the impact of climate change on yields. However, many process-based crop models use a pre-defined crop calendar based on historical observations as input (Minoli et al., 2019), where the dates of sowing and harvest are fixed and do not respond to changes in climate; this means that model projections are highly uncertain (Asseng et al., 2013). Although some crop models include crop-specific climatic requirements for sowing (Waha et al., 2012) or a relationship between sowing dates and climate (van Bussel et al., 2015), these empirical relationships are based on limited observations and their universality has not been rigorously tested (Sacks et al., 2010). The use of pre-defined crop calendars or empirical relationships stems from an imperfect understanding of the role of climate in determining sowing dates for optimal production and thus limited ability to model this dynamically (Dobor et al., 2016). However, a model which simulates optimal sowing dates given specific climate conditions is vital to provide information to help farmers adapt effectively to anticipated climate changes, and thus to contribute to global food security.

Eco-evolutionary optimality (EEO) approaches (Harrison et al., 2021), which assume that plants adjust to environmental conditions both in the short term (hours to days) and on longer timescales (seasonal to decadal) to maximum their growth (and hence reproductive fitness), have been used to simulate plant growth, both of natural systems (Mengoli et al., 2022; Tan et al., 2021) and crops (Qiao et al., 2020; Qiao et al., 2021). Many previous studies show that EEO concepts provide the basis for robust models of ecosystem processes with minimal parameter requirements (Harrison et al., 2021; Jiang et al., 2020; Mengoli et al., 2022; Tan et al., 2021) and this could reduce the level of uncertainty currently associated with the parameterization of process-based crop models.

In this paper, we develop and test an optimality-based approach to determining optimal sowing dates as a function of climate conditions and on the assumption that farmers would adopt these optimal sowing dates to maximise yields. We first improve the phenological module in an EEO-based wheat growth model (the PC model: Qiao et al., 2020; Qiao et al., 2021) to predict wheat maturity as a function of climate. We then develop a scheme to determine the season and time window for wheat sowing based on climate conditions, specifically constraints imposed by low temperature and by rainfall intensity. We run the improved PC model starting from every possible sowing date during this time window to determine which specific date gives the highest yield in each location to identify the optimal sowing date. We compare our predictions of optimal sowing dates with recent census-based observations. Finally, we predict changes in optimal wheat sowing dates under two future climate scenarios.

2. Methods and materials

2.1. The PC model

The original version of the PC model predicts wheat growth and yield using three separate modules for phenological development, carbon assimilation and carbon allocation (Qiao et al., 2020; Qiao et al., 2021). The phenological development module was adapted from the global vegetation model LPJmL4 (Schaphoff et al., 2018), which simulates wheat growth with a phenological scalar (f_{PHU}) that ranges from 0 at sowing to 1 at harvest. The f_{PHU} is temperature-dependent and is calculated as the fraction of accumulated temperature to potential heat requirements (PHU, °C days) from sowing to harvest:

$$f_{PHU} = \sum_{1}^{i}(T - T_b) \bigg/ PHU \tag{1}$$

where i is number of days after wheat sowing, T is air temperature (°C), and T_b is the lowest threshold of temperature for wheat growth. In the original version of PC model, the value of PHU was calculated based on prescribed sowing and harvest dates (Qiao et al., 2020). The

phenological module also provides a scheme to predict the dynamics of leaf area index (LAI). This scheme allows potential maximum LAI over the wheat growing period to be interpolated to daily LAI, with leaf development determined by the phenological scalar f_{PHU}. The potential maximum LAI is derived based on a mass-balance principle which takes into account both carbon limitation and water limitation, and is the lesser of a carbon- and water-limited value (Qiao et al., 2021).

The second module predicts wheat carbon assimilation using an EEO-based gross primary production (GPP) model (P model: Stocker et al., 2020; Wang et al., 2017b), which derives GPP from climatic variables and CO_2 concentration. The P model combines the Farquhar-von Caemmerer-Berry C_3 photosynthesis model (Farquhar et al., 1980) with two EEO hypotheses: the 'least-cost' (Prentice et al., 2014) and the 'coordination' (Wang et al., 2017b) hypotheses, which allow the acclimation of stomatal behaviour and carboxylation to environmental variations at weekly to monthly time scales to be taken into account (Harrison et al., 2021; Jiang et al., 2020; Wang et al., 2017b).

The third module predicts the allocation of assimilated carbon to aboveground biomass (AB), and then yield, using an empirical allocation scheme developed using global wheat observations (Qiao et al., 2020; Qiao et al., 2021). A variable fraction of assimilated carbon is allocated to AB, where this fraction is determined by soil moisture conditions indexed by the ratio of actual to equilibrium evapotranspiration (Qiao et al., 2021). Grain yields are then derived from AB based on a saturating yield allocation equation fitted to data by non-linear regression with cultivars as a random effect.

The development of the PC model to improve the prediction of wheat phenology, appropriate sowing season and optimal sowing dates are described in Sections 2.3 and 2.4 below.

2.2. Data description

Various different datasets were used for model improvement, to drive model simulations, and for subsequent evaluation. Wheat phenological observations and high-resolution temperature data were used to derive the response of PHU to environmental factors. Global data on climate variables, CO_2 concentration, wheat-growing areas and the location of irrigated wheat were used to drive PC model simulations. Census-based data sets on wheat sowing dates and wheat potential yield globally were used to assess the PC model predictions.

2.2.1. Data for model development

A global dataset of wheat phenological observations at individual sites, including wheat sowing and harvest dates, was compiled from the Pan European Phenology project (Templ et al., 2018), the Chinese Meteorological Administration (CMA: www.nmic.cn/data), the Kellogg Biological Station (KBS: www.lter.kbs.msu.edu) and from published papers (Table S1). The dataset includes 7106 agricultural sites located in the major wheat planting regions of the world (Fig. S1) and contains 81,005 site-years of phenological observations. This global dataset of wheat sowing and harvest dates was used to determine the wheat growing period required to calculate the potential heat requirements (PHU) over the growing period.

We derived temperature data from two data sets: CHELSA-W5E5 and E-OBS. The CHELSA-W5E5 dataset (Karger et al., 2021) is global in extent and has a spatial resolution of ~1 km (30 arcsec) with daily temporal resolution from 1979 to 2016. Some of the European sites had phenological observations spanning a longer interval, and we extracted temperature data for these sites and times from the E-OBS gridded dataset (Cornes et al., 2018). The E-OBS dataset provide information for Europe at a coarser resolution (0.1°) than CHELSA-W5E5 but has daily temporal resolution from 1950 to the present.

2.2.2. Input data for global simulations

For the simulations of historical (2000 CE) wheat sowing dates, we obtained climatic variables from WFDE5 (Cucchi et al., 2020) at a spatial

resolution of 0.5° between 1990 and 2000, specifically 2 m air temperature (T, °C), atmospheric pressure (P_{air}, Pa), 2 m specific humidity (SH, kg kg^{-1}), downward shortwave radiation flux (R_{sw}, W m^{-2}), and precipitation (rain and snowfall) rate (P, kg m^{-2} s^{-1}). The WFDE5 data are at hourly temporal resolution and a daily value was calculated as the mean of the hourly data over 24 h. For the simulations of the changes in wheat sowing dates under future scenarios, the same climatic variables between 2015 and 2100 were extracted from bias-corrected CMIP6 climate forcing provided by protocol 3b (Lange and Büchner, 2022) of The Inter-Sectoral Impact Model Intercomparison Project (ISIMIP-3b). These climatic variables are at a spatial resolution of 0.5° and a daily temporal resolution. ISIMIP-3b provides climate forcing for three future scenarios (SSP126, SSP370 and SSP585), including five primary CMIP6 climate models (GFDL-ESM4, MPI-ESM1-2-HR, MRI-ESM2-0, IPSL-CM6A-LR and UKESM1-0-LL). We considered only two scenarios (SSP126 and SSP370) as SSP585 is now considered implausible (Hausfather and Peters, 2020).

We used these daily data to compute the variables required by the PC model: vapour pressure deficit (VPD, Pa) and daily photosynthetic photon flux density (PPFD, μmol m^{-2} s^{-1}). VPD was calculated as the difference between saturated vapour pressure and actual vapour pressure using 2 m air temperature, atmospheric pressure and 2 m specific humidity (Allen et al., 1998). PPFD was calculated from downward shortwave radiation as PPFD $= 3600 \times 24 \times 10^{-6} R_{sw} k_{EC}$, where $k_{EC} = 2.04$ μmol J^{-1} (Meek et al., 1984) converts energy units (W m^{-2}) to photon flux units (μmol m^{-2} s^{-1}). The daily variables were preprocessed to provide weekly inputs for the PC model. The weekly inputs were the averages of the daily variables, except for PPFD which was summed over the week. The global annual average CO_2 concentration for each year was obtained from the US National Oceanic and Atmospheric Administration (NOAA: www.esrl.noaa.gov).

The wheat-growing areas were defined from the EARTHSTAT wheat distribution map (www.earthstat.org), which was created by merging census data with satellite-derived datasets (Ray et al., 2012). EARTHSTAT provides the ratio of wheat areas harvested in each grid cell at spatial resolution of ~0.083° and we resampled the spatial resolution to 0.5°. Information on whether the wheat was irrigated or not was derived from the MIRCA2000 dataset (Portmann et al., 2010), which provides the area of irrigated and rainfed wheat in each 0.5° grid cell where wheat is grown. In grid cells with both irrigated and rainfed wheat, we used the dominant type. Thus, if the ratio of irrigated to rainfed wheat in any grid cell is >0.5, we assumed for modelling purposes that all the wheat in that grid cell is irrigated.

2.2.3. Model evaluation data

We used two widely used global sources of data on wheat sowing dates, MIRCA2000 (Portmann et al., 2010) and Sacks et al. (2010), as a basis for creating a dataset to evaluate PC model simulations. Both data sets provide information on a 0.5° grid for the period around 2000 CE. The MIRCA2000 dataset gives the typical month of wheat sowing for rainfed and irrigated wheat separately and also the area of wheat planted in each month. The Sacks et al. (2010) data set gives information about the length of the sowing period (including start date, dominant sowing time and end date) for spring and winter wheat separately, but does not separate rainfed and irrigated wheat. Both data sets use census data from FAO and USDA, but differ in the sources of information used at sub-national scale.

There are differences between the two data sets in the area where wheat is grown, in part because the Sacks et al. (2010) data sets assumes that wheat was grown in all grid cells within a sub-national administrative unit. Although MIRCA2000 provides the planted area in each grid cell, the relatively coarse resolution means that there are differences between this data set and the wheat-growing areas delineated in the higher resolution (~0.083°) EARTHSTAT data set. We assumed that the distribution of wheat-growing areas in EARTHSTAT was more reliable. By comparing EARTHSTAT to the two wheat calendar maps, we

identified grid cells erroneously indicated as places where wheat was grown (Fig. S4) and removed these grid cells from the final data set. We also identified places where there were inaccuracies in the wheat sowing dates given in MIRCA2000 and Sacks et al., particularly for parts of Russia, China and South America (Fig. S5b). We used country-specific information from published papers and reports to correct these errors (Table S2). The details of the correction procedure are given in Text S1 and Fig. S3. We used the data set produced after these corrections (Fig. S5d) to validate PC model predictions of optimal wheat sowing dates globally.

EARTHSTAT also provides gridded estimates of potential wheat yield at ∼0.083° spatial resolution for the period around 2000 CE (Mueller et al., 2012). Potential wheat yield was derived from the global gridded dataset of actual wheat yield based on climate zones defined by growing degree days and a soil moisture index. Within each climate zone, potential yield was estimated as the 95% quantile of all the actual yield data. We aggregated this dataset from ∼0.083° to the 0.5° grid by weighting the wheat area in each grid and used this aggregated dataset to evaluate model predictions of potential wheat yield.

2.3. The new phenological module

In this study, we extended the original phenological module by improving the presentment of PHU to offset the dependency on wheat calendar and simulate this value based on the response of PHU to environmental factors. The length of the wheat growing period (from sowing to harvest) is determined by the sowing date and the accumulated heat requirement for wheat maturity. However, photoperiod and accumulated chilling also affect wheat phenology and influence the PHU required to reach maturity. We used day length (DL, hours) and the number of days with temperature below 5 °C (DayBelow5, days) to represent photoperiod and chilling accumulation, respectively. We assumed a linear response of PHU to these two factors as follows:

$$PHU = f_{DL} \, DL + f_{DayBelow5} \, DayBelow5 + \partial \qquad (2)$$

where PHU is the potential heat requirement, DL is the day length, DayBelow5 is the number of days with temperature below 5 °C, f_{DL} and $f_{DayBelow5}$ are the sensitivity to DL and DayBelow5, respectively, and ∂ is a intercept.

We used the global wheat phenological observations dataset to determine the wheat growing period and calculated PHU, DL and DayBelow5 based on wheat growing period, site location and air temperature. The PHU observations for each site-year were calculated as the sum of the difference between air temperature (T) and the baseline temperature (T_b) over the wheat growing period:

$$PHU = \sum_{1}^{L}(T - T_b) \qquad (3)$$

where L is the length of growing period. DL was calculated using the daylength function in the R package "*geosphere*" based on the latitude of each site and sowing date in each year. DayBelow5 was calculated from the first day with temperature below 5 °C to the last day with temperature below 5 °C, using a 7-day moving average to minimise the effect of short-term temperature fluctuations.

We performed OLS regression on PHU, DL and DayBelow5 to estimate the parameters f_{DL}, $f_{DayBelow5}$ and ∂ in Eq. (2) for winter wheat and f_{DL}, and ∂ for spring wheat, respectively. We included separate PHU response equations to predict wheat maturity for winter and spring wheat. Specifically, we predicted PHU for winter wheat accounting for dormancy as:

$$PHU = 135.54DL - 7.7DayBelow5 + 1932.7 \qquad (4)$$

PHU was predicted for spring wheat, which does not have a dormancy requirement, as:

$$PHU = -197.79DL + 4479.1 \qquad (5)$$

2.4. Prediction of optimal wheat sowing dates

2.4.1. Determination of sowing season

We used mean monthly temperature of the coldest month (MTCO) and rainfall seasonality (represented by the difference between maximum monthly rainfall and minimum monthly rainfall, DI) to determine whether wheat would be planted in autumn or spring. We used an MTCO threshold value of −10 °C to determine areas where cold damage would exclude autumn sowing and an MTCO threshold value of 5 °C where autumn sowing would be precluded because of dormancy constraints. The low MTCO threshold reflects physiological constraints on wheat survival and the high MTCO threshold was determined according to Waha et al. (2012) as the temperature threshold for the sowing of spring wheat. This results in three temperature seasonality categories: cold regions, characterized by MTCO less than −10 °C; temperate regions, characterized by MTCO above −10 °C but less than 5 °C; warm regions, characterized by MTCO above 5 °C. Temperature is not a constraint on wheat growth in warm regions, but some of these regions are characterized by monsoonal climates where heavy rainfall could damage the crop and sowing generally occurs after the monsoon. We therefore subdivided the warm regions to separate out monsoon regions, using a DI threshold of 150 mm recommended by Sperber et al. (2013) and defining the monsoon season as the period when the relative rainfall exceeds 5 mm day^{-1}.

According to the sowing season, we determined the suitability of climate conditions for wheat sowing. In cold regions, wheat is sown in late spring and summer to avoid frost damage. Wheat sown in these regions does not undergo dormancy, and the growing period finishes when the requirement of accumulated temperature is satisfied. In temperate regions, low winter temperatures induce dormancy. Wheat can be planted at any time the temperature exceeds the dormancy threshold, but wheat sown before the winter will undergo dormancy under low temperature while wheat sown in spring will not. In warm regions, temperature does not constrain the sowing date, but in monsoon regions, where heavy rainfall would damage the plants, wheat is sown when the summer monsoon retreats.

We calculated the average of MTCO and DI from 1990 to 2000 based on gridded climatic data at 0.5° resolution obtained from WFDE5. The global geographic variation of MTCO and precipitation over year are shown in Fig. S2. Frequency distributions of MTCO and precipitation in climatic space are also shown in Fig. S2.

2.4.2. Determination of optimal sowing dates

We assumed that optimal sowing dates correspond to maximum grain yields, and estimated optimal sowing dates as follows: (1) we assumed that wheat could be sown at any time when the climate conditions are suitable and would be harvested when the potential heat requirements (PHU) required are reached; (2) we then calculated the grain yields corresponding to every potential sowing date. To examine the impact of the low temperature and rainfall intensity constraints, we ran three simulations: (1) without any additional constraint; (2) with the MTCO constraint and (3) with both the MTCO and the rainfall intensity constraint.

2.5. Prediction of the changes in optimal wheat sowing dates under future scenarios

We calculated the mean value of each climate variables among five primary climate models included in ISIMIP-3b for the two future scenarios considered. The mean climate forcing was used as the inputs of PC model. We ran full simulations (with both the MTCO and rainfall intensity constraint) to predict the optimal wheat sowing dates corresponding to maximum grain yields from 2015 to 2100. The changes in

wheat sowing dates were calculated as the differences between the predicted wheat sowing dates in a given year and 2000 CE.

2.6. Prediction of potential yield driven by optimal sowing dates

We ran the PC model firstly using our revised census-based sowing dates and secondly the predicted optimal sowing dates, but keeping all other inputs the same, to predict potential wheat yield globally in 2000 CE. We compared the spatial patterns of these two predictions with the EARTHSTAT benchmark for potential wheat yield and also compared them each other to test the positive impacts involved in optimal sowing dates.

3. Results

3.1. The response of PHU to environmental factors

Photoperiod (represented by DL) and chilling accumulation (represented by DayBelow5) explain ~59% variation of the PHU for winter wheat (Fig. 1). Chilling accumulation reduces the thermal requirements for maturity in winter wheat. DL explains ~41% of the variation in PHU for spring wheat. The response of PHU to daylength is positive for winter wheat, and negative for spring wheat.

3.2. Prediction of the wheat sowing season

The predicted distribution of wheat growing season, based on temperature limits and rainfall intensity, broadly matches the observed spatial distribution of winter and spring wheat types (Fig. 2 and S4).
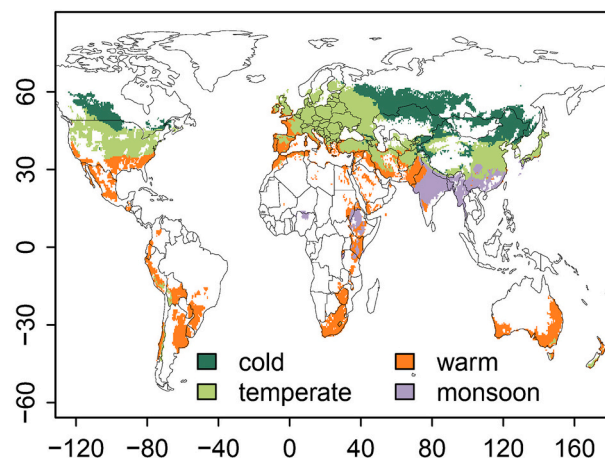

Fig. 2. Global distribution of seasonality types. Seasonality types are based on the annual pattern of temperature and precipitation. Cold regions are characterized by MTCO <-10 °C; temperate regions are characterized by MTCO >-10 °C but <5 °C; warm regions are characterized by MTCO >5 °C; monsoon regions are characterized by MTCO >5 °C with significant monsoon cycles. Regions shown in white are areas where wheat is not grown. The predicted distribution can be compared to the observed census-based distribution (Fig. S4).

Cold regions are entirely dominated by spring wheat. Temperate regions are mostly characterized by winter wheat, although discrepancies between the predicted and observed distribution occur where spring wheat
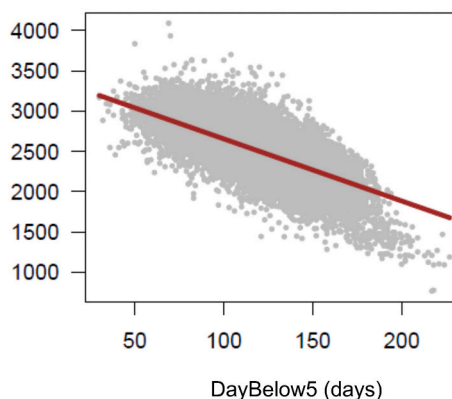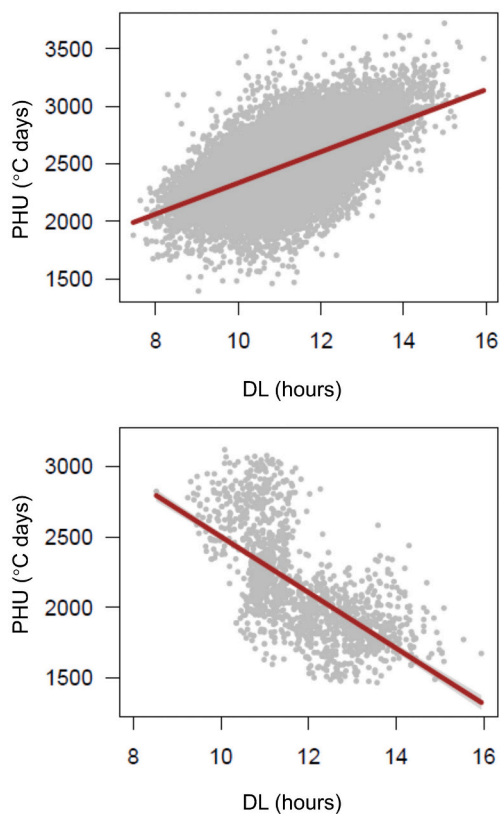
	DL	DayBelow5	intercept	R^2
WW	135.54	−7.7	1932.7	0.59
SW	−197.79	0	4479.1	0.41

Fig. 1. The response of potential heat requirements to environmental variables. The top two scatterplots show the response of winter wheat. The bottom scatterplot shows the response of spring wheat. The sensitivity of each wheat type for each environmental variable is shown in the table. PHU is the accumulation of temperature above 0 °C from sowing to harvest. DL is the day length when wheat is planted, calculated based on latitude and days of year. DayBelow5 is the number of days with temperature <5 °C from wheat sowing to harvest. Winter wheat (WW) is a type of wheat that requires dormancy when the temperature is below the temperature threshold. Spring wheat (SW) is a type of wheat that does not require dormancy. Here, MTCO over wheat growing period is used to separate winter wheat (MTCO <5 °C) and spring wheat (MTCO >5 °C).

is sown as part of a crop rotation. Both spring wheat and winter wheat can be grown in warm regions, but the inclusion of the rainfall intensity constraint is important in monsoon regions.

3.3. Prediction of optimal wheat sowing dates

We compared the three PC model simulations with the observations of wheat sowing dates (Fig. 3). The original version of the model, without MTCO and rainfall intensity constraints, reproduces the spatial
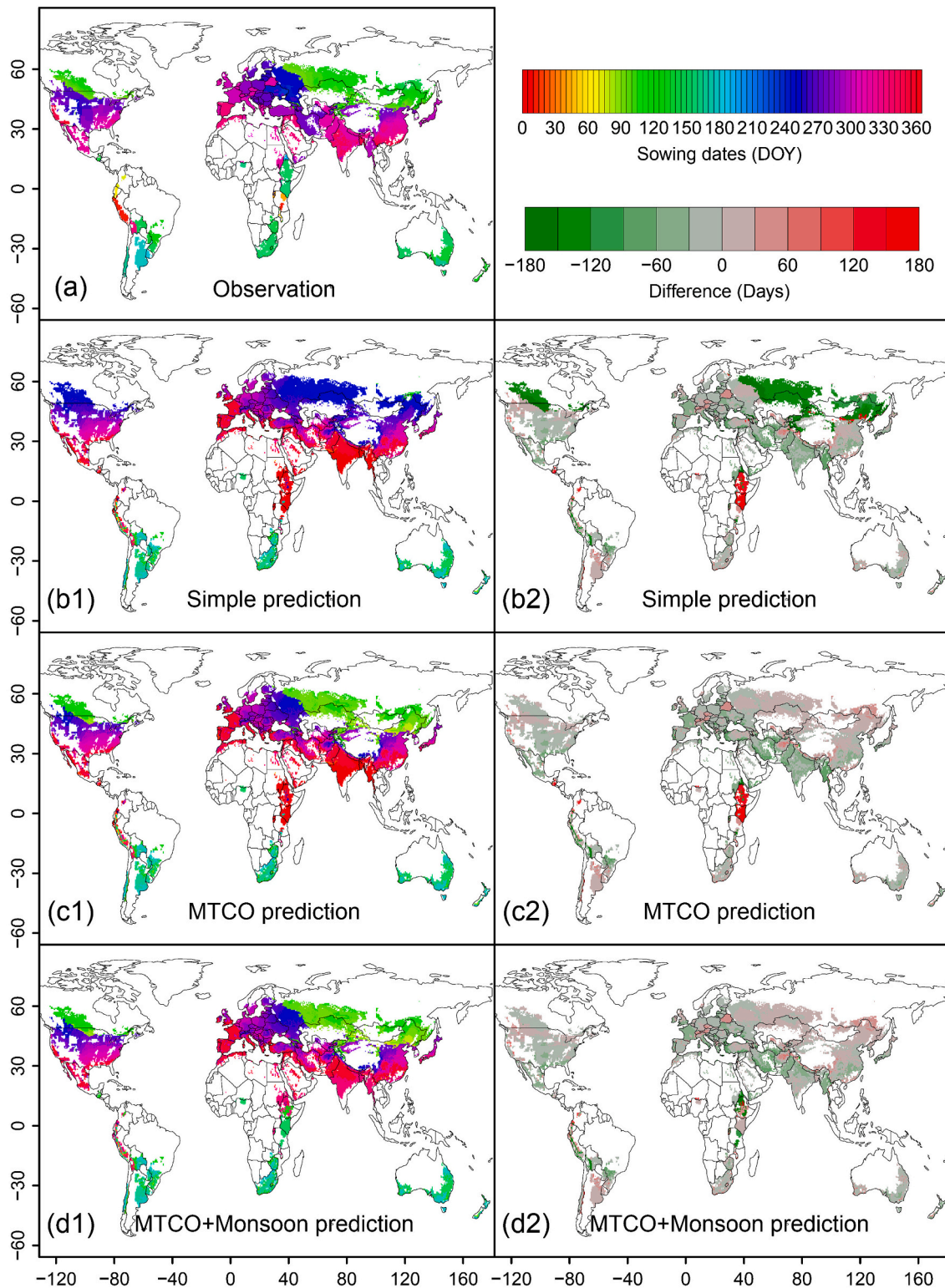

Fig. 3. Comparison of predicted wheat sowing dates with observed wheat sowing dates. (a) corrected census-based wheat sowing dates; **(b1)** prediction without any additional constraints; **(c1)** prediction with the constraint based on the monthly temperature of the coldest month (MTCO). **(d1)** prediction considering both the rainfall intensity and MTCO constraint. **(b2, c2 and d2)** show the differences between the observations and predictions for each model.

patterns in temperate and warm regions (Fig. 3a and b1), but not in cold regions and most monsoon regions (Fig. 3b2). The predicted optimal wheat sowing dates in cold regions are from August to September, whereas the observations show sowing dates around April. In monsoon regions, the predicted sowing date is around the start of the monsoon season (Fig. S6), whereas the observed sowing dates are at the end of the monsoon season. The failure of the model in these regions confirms that it is necessary to include some additional constraint to improve the
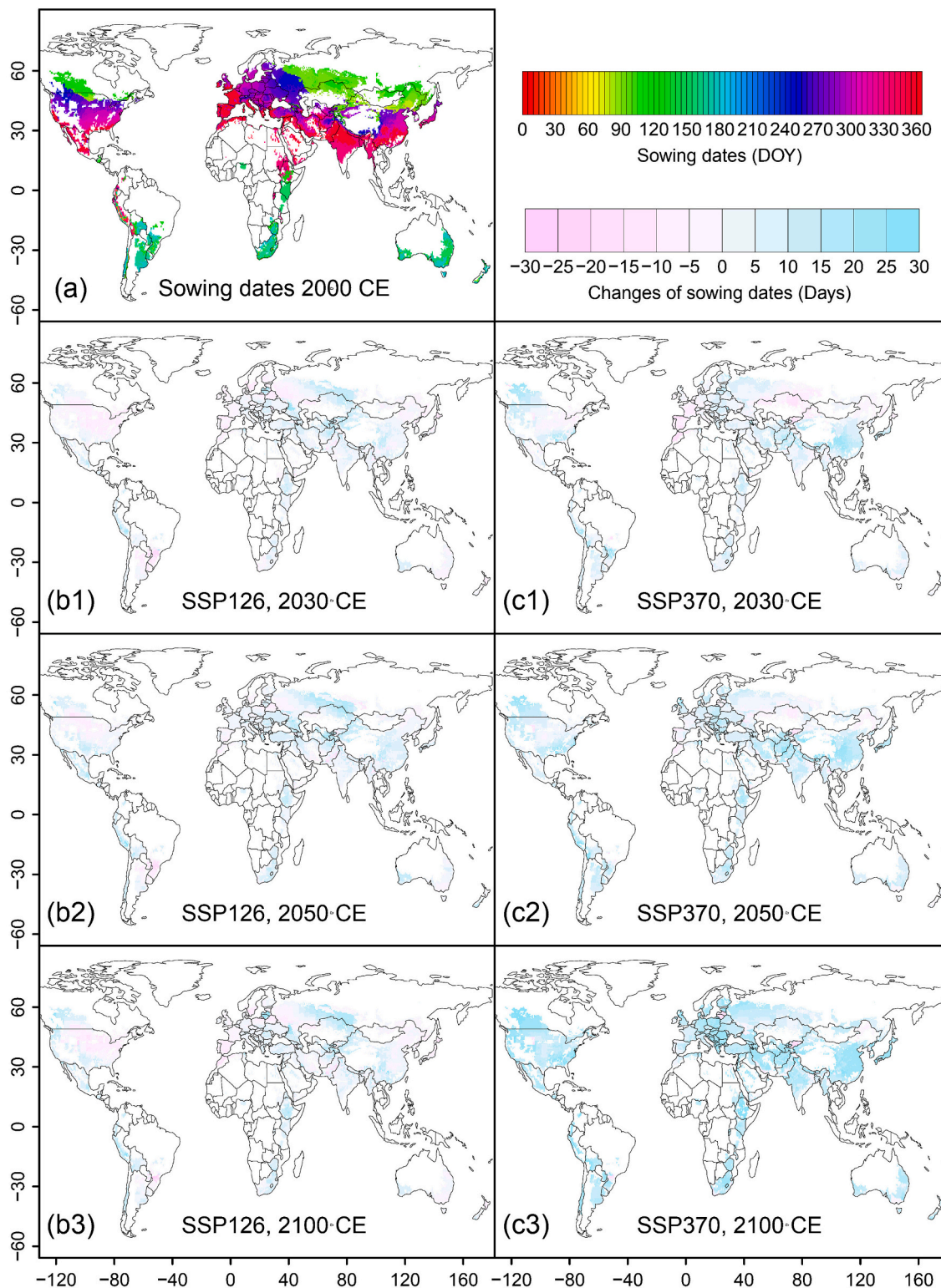

Fig. 4. Predicted changes in optimal wheat sowing dates under two future scenarios. (a) wheat sowing date prediction in 2000 CE, as in Fig. 3d1; **(b1-b3)** predicted changes under SSP126 compared with 2000 CE; **(c1-c3)** predicted changes under SSP370 compared with 2000 CE. Changes are expressed as ten-year averages (2020–2029 for 2030 CE, 2040–2049 for 2050 CE and 2090–2099 for 2100 CE). Negative values indicate advanced sowing dates, positive values indicate delayed sowing dates.

prediction. Inclusion of the MTCO constraint improves the realism of the simulation in cold regions (Fig. 3c1 and c2) and the inclusions of a rainfall intensity constraint improves the realism of the simulation in monsoon regions (Fig. 3d1 and d2), respectively. Predicted sowing dates in cold regions are around April, as observed, and the difference in timing between predictions and observations is reduced from more than 120 days to less than 30 days. In monsoon regions, the difference in timing between predictions and observations is reduced from around 150 days to around 30 days. Differences between estimated and observed sowing dates in the final model are less than one month ($<$ 30 days) over most of the world (Fig. S7). Maximum errors occur in tropical regions with large altitudinal gradients, such as Ethiopia, Bolivia and Peru, where the difference between predicted and observed sowing dates can be up to two months (Fig. 3d2).

3.4. Changes in optimal wheat sowing dates under future scenarios

Climate change will affect the global pattern of optimal wheat sowing dates in the future (Fig. 4). Under the most "optimistic" scenario (SSP126), global average temperatures increase slightly (no more than 2 °C) until the 2050s and then slowly decline (Fig. S9). Predicted optimal wheat sowing dates are advanced in most wet areas (e.g. central and eastern North America, western Europe, northeastern China and eastern Australia) but delayed in areas with less water availability (e.g. central and western Asia, northern and northwestern China, western Australia, East Africa and some areas in Latin America). Similar variations are found in the historical wheat sowing records (Collins and Chenu, 2021; Ding et al., 2016; Fatima et al., 2020; Stephens and Lyons, 1998). Higher temperatures are more likely to lead to later wheat sowing dates (Fig. 4b2, compared to b1 and b3). The fraction of grid cells with delayed sowing dates increases with warming (Fig. S10). Under the SSP126 scenario, grid cells with advanced sowing dates are dominant ($>$ 50%) in the early 21st century, but as time goes on, grid cells with delayed sowing dates begin to dominate. In the late 21st century, grid cells with advanced sowing dates reassert dominance (Fig. 4b1-b3 and Fig. S10a).

Under the more "pessimistic" scenario (SSP370), global average temperatures rise rapidly (exceeding 5 °C by 2100, Fig. S9). Predicted optimal wheat sowing dates are delayed in most regions (Fig. 4c1) except for very limited areas (the extremely humid winter wheat zones, for example, in western Europe and mid-eastern North America; and some cold regions where wheat is sown in spring, for example, in northwestern China, Kazakhstan and some Russian regions bordering Kazakhstan) in the early 21st century (Fig. 4c1). The delays are furtherly enhanced with increasing temperature (Fig. 4c3, compared to c2 and c1). By the end of 21st century (Fig. 4c3), predicted optimal sowing dates in almost all areas are delayed to some extent, by around 20 days. The statistics (Fig. S10b) show that grid cells with delayed sowing dates are dominant (already $>$50% in the early 21st century, and increasing over time to $>$80% by the end of 21st century) under the SSP370 scenario.

3.5. Prediction of potential yield

The simulation of wheat potential yield captures the spatial patterns and also the magnitude of potential wheat yield as shown by EARTH-STAT. Both identify regions with high potential yield ($>$6 t ha^{-1}) in northern China, western Europe and eastern North America. They also agree on regions with low potential wheat yield ($<$3 t ha^{-1}) in Russia, central America and parts of Australia. The pattern of the prediction driven by optimal sowing dates is similar to the prediction driven by revised census-based sowing dates in spatial pattern, but slightly larger in magnitude (Fig. S8). The increase in potential yield is more pronounced ($>$1 t ha^{-1}) in regions with favorable climate conditions or intensive irrigation, such as Europe, eastern North America and northern China. The differences between the two simulations are smaller

($<$0.5 t ha^{-1}) in regions of rainfed wheat such as central Asia and central America. Higher yields driven by optimal sowing dates implies the potential of adjusting sowing dates to mitigate the adverse effects of future climate change.

4. Discussion

We have shown that the inclusion of constraints associated with winter chilling and photoperiod are necessary to estimate PHU correctly. The importance of these two environmental factors for thermal requirements has been shown from agronomic experiments (Aslam et al., 2017; Villegas et al., 2016). Chilling reduces the PHU requirement to reach maturity in winter wheat. However, photoperiod has opposite effects on winter and spring wheat, increasing PHU for winter wheat and decreasing PHU for spring wheat. Wheat is a long-day plant and the physiological development rate is accelerated by higher temperatures corresponding to extended daylength (Sheehan and Bentley, 2021). This explains why spring wheat requires less PHU to reach maturity when it is sown later in the spring. However, winter wheat is responsive to vernalization, which requires a period of cold days, to make the transition from vegetative to reproductive development (Hyles et al., 2020; Sheehan and Bentley, 2021). Winter wheat sown earlier in the autumn, with longer daylength, will remain vegetative until the vernalization requirement has been satisfied (Sheehan and Bentley, 2021). This delays reproductive development, so that a greater thermal accumulation is required to reach maturity. In addition, saturation of vernalization is the prerequisite for winter wheat to flower, which reduces the time to flowering (Eagles et al., 2009; Hyles et al., 2020; Trevaskis, 2010). This explains why chilling accumulation, an index for vernalization, reduces the PHU required to reach maturity in winter wheat.

Additional constraints are required to predict the optimal sowing season, specifically winter temperature and rainfall intensity. Previous studies confirm that temperature is important because of threshold requirements for dormancy and vernalization (Waha et al., 2012) as well as for minimising the possibility for frost damage (Kotsuki and Tanaka, 2015). In addition to the direct damage caused by heavy rain (Mathison et al., 2018), intense rains can impede physiological processes such as flowering (Chen et al., 2020; Flohr et al., 2017) and pollination (Zhang et al., 2016). We have shown that low temperatures, as indexed by MTCO below -10 °C, are sufficient to exclude the growth of winter wheat and favour the sowing of spring wheat as observed in these cold regions. We have also shown that the timing of sowing in regions with high rainfall seasonality, such as tropical regions with monsoon climates, is optimised to ensure that plants are not damaged by heavy rains. Including a rainfall seasonality threshold allows us to predict that the optimal sowing season is during the retreat of the monsoon, as observed. This confirms the hypothesis that the sowing dates adopted by farmers are generally approximately optimal for local climatic conditions, an idea which underpins the use of a crop calendar for modelling but has not been extensively tested (Lilley et al., 2019; Stehfest et al., 2007).

We have used the improved PC model, incorporating these constraints, to predict optimal sowing dates for wheat as a function of climate. Comparison with observed sowing dates show that the model reproduces the observed timing of sowing reasonably well, with differences that are less than 30 days across most of the world. Differences are largest in regions where the temperature seasonality is small and soil moisture conditions are favorable for wheat growth throughout the year. Then the wheat sowing season can span a long period (Iizumi et al., 2019) and, since the farmers are mostly smallholders (Cohn et al., 2017), the timing of sowing is influenced by individual decisions and resources (Gollin, 2014). These are also regions where multiple crops are grown in the year, so that the aim is to maximise the total yield of all crops and the sowing of wheat may therefore not always be at the optimal time for that crop alone. Substantial differences between model predictions and census-based observations of sowing dates are also found in regions with

large differences in climate associated with elevation. These differences are likely due to the fact that the census-based observations are based on information at the scale of an administrative unit and do not capture the variability in climate, and therefore sowing dates, in regions with high topographic diversity (Kotsuki and Tanaka, 2015).

Optimal sowing dates are predicted here to change considerably under future scenarios. Early sowing can extend the growth period of wheat to some extent, but it can also lead to moisture stress because spring and autumn are not moisture-rich seasons for wheat cultivation in most wheat-growing regions (Fatima et al., 2020; Ren et al., 2019). Therefore, there is a need to balance water availability with the extension in the length of the growth season (Fatima et al., 2020; Liu et al., 2018). Slight warming (SSP126) favors earlier wheat sowing in areas with good water availability, to offset the effects of faster phenological development (Wang et al., 2020); but delays optimal wheat sowing in drier regions where it is critical to ensure that key physiological stages, including flowering and grain filling, occur in a period with enough water (Fatima et al., 2020). However, large warming (e.g. SSP370) generally leads to a delayed optimal sowing date, for two reasons. Firstly a large warming, on the one hand, exacerbates water stress on wheat growth and, on the other hand, accelerates phenological development, shortening the growth season. Delaying the sowing date shifts the growing season to a period of stronger radiation and more precipitation, offsetting to some extent the negative impact of warming on yield (Fatima et al., 2020). Secondly, for winter wheat, the temperature should drop to a certain threshold before sowing in autumn (Sacks et al., 2010). The prediction of changes in optimal wheat sowing dates in this study involves a balance among multiple climatic variable to ensure the highest wheat yields, suggesting a key role for phenological adjustment in mitigating the potentially adverse effects of climate change.

The comparison of PC model predictions of potential yield compares well with the EARTHSTAT observations of potential yield in 2000 CE, both in terms of spatial patterns and in overall magnitude. This suggests that the adoption of an EEO-based approach to simulating crop yield could substantially reduce the current uncertainty of assessments of the impact of future climate changes on crops. It would be useful to extend this approach to other major crop types, given its relative simplicity.

Climate change is already affecting regional climates and is seen as a threat to global food security (Hasegawa et al., 2018; Rosenzweig et al., 2014). Global warming is already having adverse effects on wheat production, including shortening the life cycle (Farooq et al., 2011; Lobell et al., 2012), increasing stress during the growing season (Tack et al., 2015), decreasing grain yield (Lesk et al., 2021; Perry et al., 2020), and increasing damage by pests and diseases (Deutsch et al., 2018; Wang et al., 2022). Increases in precipitation variability are also having adverse effects on wheat yield (Feng et al., 2018; Latiri et al., 2010). The adaption of management strategies, such as increasing irrigation or using cultivars with high heat-tolerance, are one way of mitigating the impacts of climate change (Aggarwal et al., 2019; Beveridge et al., 2018), but such technological solutions raise the cost of crop production and the benefits vary depending on local climate and soil conditions. Adjusting sowing dates to ensure that key physiological stages, such as flowering and grain filling, occur in the optimal window (Flohr et al., 2017) under a changing climate could provide an alternative way to combat the negative effects of climate change (Sandhu et al., 2020). Indeed, studies have shown that changes in sowing dates can prolong wheat growth (Mueller et al., 2015) and boost wheat yield (Hunt et al., 2019) despite ongoing climate change. Recent shifts in observed sowing dates (Lobell et al., 2013; Olesen et al., 2012) suggest that farmers are already adjusting their management practices in this way. However, it is unclear whether changes in the season of sowing will be required or indeed whether sufficient adjustments could be made to sowing dates to cope with future climate changes. Crop models that impose a plant calendar are obviously not ideal for investigating this, but the optimality-based approach used in the PC model could be used to predict optimal wheat sowing dates under different future climate scenarios and

thus provide a more secure basis for assessments of the need and potential of changing management practices to mitigate the negative impacts of climate change on crop growth.

5. Conclusions

The thermal requirements for wheat maturity are affected by photoperiod and chilling accumulation, with different responses to photoperiod depending on whether vernalization and dormancy are required. Our optimality-based modelling approach including these two constraints, and reproduces both the observed spatial patterns for the timing of sowing and the spatial patterns and magnitude of potential wheat yield in the 2000 CE benchmark provided by EARTHSTAT. Our predictions under future scenarios indicates that optimal dates for wheat sowing will become earlier in wet areas but later in dry regions under slight warming, while greater warming favors delayed wheat sowing in most of the current wheat-growing areas. The good performance of the revised PC model suggests that this approach could be used to estimate optimal sowing times for crops in response to future climate change scenarios, and thus provide a basis for farmers to adjust their management practices to optimise yields in a changing climate.

Author contributions

SCQ collected the data supporting this study. SCQ carried out the analyses and prepared the display items with contributions from SPH, ICP and HW. SCQ wrote the first draft. SPH, ICP and HW contributed to the revision. All authors contributed to the interpretation of the results.

Declaration of Competing Interest

The authors declare that they have no competing interests.

Data availability

The global wheat phenological observations used for improving phenological scheme were obtained from the Pan European Phenology project (https://www.pep725.eu), the Chinese Meteorological Administration (https://www.nmic.cn/data), the Kellogg Biological Station (https://www.lter.kbs.msu.edu) and from published papers (see Table S1). The high-resolution temperature data used for deriving the response of potential heat requirements (PHU) to environmental factors were extracted from two data sets: CHELSA-W5E5 (https://doi.org/10.48364/ISIMIP.836809.1) and E-OBS (https://www.ecad.eu/download/ensembles/download). The climate data used for global simulation was obtained from WFDE5 (https://doi.org/10.24381/cds.20d54e34) for historical simulations and from the Inter-Sectoral Impact Model Intercomparison Project-3b (https://www.isimip.org) for future scenarios. The global annual average CO_2 concentration for each year was obtained from the US National Oceanic and Atmospheric Administration (https://www.esrl.noaa.gov). The global wheat distribution map was downloaded from the EARTHSTAT archive (https://www.earthstat.org). The census-based wheat sowing dates used for model evaluation were from MIRCA 2000 (https://www.uni-frankfurt.de/45218023/MIRCA) and the dataset produced by Sacks et al. (https://sage.nelson.wisc.edu). The benchmark data for potential yield were obtained from EARTHSTAT.

Appendix A. Supplementary data

Supplementary data to this article can be found online at https://doi.org/10.1016/j.agsy.2023.103608.

References

Aggarwal, P., Vyas, S., Thornton, P., Campbell, B.M., 2019. How much does climate change add to the challenge of feeding the planet this century? Environ. Res. Lett. 14 (4), 043001.

Agnolucci, P., et al., 2020. Impacts of rising temperatures and farm management practices on global yields of 18 crops. Nat. Food. 1 (9), 562–571.

Allen, R.G., Pereira, L.S., Raes, D., Smith, M., 1998. Crop evapotranspiration-guidelines for computing crop water requirements-FAO irrigation and drainage paper 56. FAO, Rome 300 (9), D05109.

Aslam, M.A., et al., 2017. Can growing degree days and photoperiod predict spring wheat phenology? Front. Environ. Sci. 5, 57.

Asseng, S., et al., 2013. Uncertainty in simulating wheat yields under climate change. Nat. Clim. Chang. 3 (9), 827–832.

Asseng, S., et al., 2014. Rising temperatures reduce global wheat production. Nat. Clim. Chang. 5 (2), 143–147.

Beveridge, L., Whitfield, S., Challinor, A., 2018. Crop modelling: towards locally relevant and climate-informed adaptation. Clim. Chang. 147 (3–4), 475–489.

Chen, C., et al., 2020. The shifting influence of future water and temperature stress on the optimal flowering period for wheat in Western Australia. Sci. Total Environ. 737, 139707.

Cohn, A.S., et al., 2017. Smallholder agriculture and climate change. Annu. Rev. Environ. Resour. 42 (1), 347–375.

Collins, B., Chenu, K., 2021. Improving productivity of Australian wheat by adapting sowing date and genotype phenology to future climate. Clim. Risk Manag. 32.

Cornes, R.C., van der Schrier, G., van den Besselaar, E.J.M., Jones, P.D., 2018. An ensemble version of the E-OBS temperature and precipitation data sets. J. Geophys. Res.-Atmos. 123 (17), 9391–9409.

Cucchi, M., et al., 2020. WFDE5: bias-adjusted ERA5 reanalysis data for impact studies. Earth Syst. Sci. Data 12 (3), 2097–2120.

Deutsch, C.A., et al., 2018. Increase in crop losses to insect pests in a warming climate. Science 361 (6405), 916–919.

Ding, D.Y., et al., 2016. Modifying winter wheat sowing date as an adaptation to climate change on the loess plateau. Agron. J. 108 (1), 53–63.

Dobor, L., et al., 2016. Crop planting date matters: estimation methods and effect on future yields. Agric. For. Meteorol. 223, 103–115.

Eagles, H.A., Cane, K., Vallance, N., 2009. The flow of alleles of important photoperiod and vernalisation genes through Australian wheat. Crop. Pasture. Sci. 60 (7), 646–657.

Elliott, J., et al., 2014. Constraints and potentials of future irrigation water availability on agricultural production under climate change. Proc. Natl. Acad. Sci. U. S. A. 111 (9), 3239–3244.

Farooq, M., Bramley, H., Palta, J.A., Siddique, K.H.M., 2011. Heat stress in wheat during reproductive and grain-filling phases. Crit. Rev. Plant Sci. 30 (6), 491–507.

Farquhar, G.D., von Caemmerer, S., Berry, J.A., 1980. A biochemical model of photosynthetic CO_2 assimilation in leaves of C_3 species. Planta 149 (1), 78–90.

Fatima, Z., et al., 2020. The fingerprints of climate warming on cereal crops phenology and adaptation options. Sci. Rep. 10 (1), 18013.

Feng, P.Y., et al., 2018. Impacts of rainfall extremes on wheat yield in semi-arid cropping systems in eastern Australia. Clim. Chang. 147 (3–4), 555–569.

Flohr, B.M., Hunt, J.R., Kirkegaard, J.A., Evans, J.R., 2017. Water and temperature stress define the optimal flowering period for wheat in South-Eastern Australia. Field Crop Res. 209, 108–119.

Gollin, D., 2014. Smallholder Agriculture in Africa. IIED Work. Pap. IIED, London (2014).

Harrison, S.P., et al., 2021. Eco-evolutionary optimality as a means to improve vegetation and land-surface models. New Phytol. 231 (6), 2125–2141.

Hasegawa, T., et al., 2018. Risk of increased food insecurity under stringent global climate change mitigation policy. Nat. Clim. Chang. 8 (8), 699–703.

Hausfather, Z., Peters, G.P., 2020. Emissions–the 'business as usual' story is misleading. Nature 577, 618–620.

Hernandez-Ochoa, I.M., et al., 2018. Climate change impact on Mexico wheat production. Agric. For. Meteorol. 263, 373–387.

Hunt, J.R., et al., 2019. Early sowing systems can boost Australian wheat yields despite recent climate change. Nat. Clim. Chang. 9 (3), 244–247.

Hyles, J., Bloomfield, M.T., Hunt, J.R., Trethowan, R.M., Trevaskis, B., 2020. Phenology and related traits for wheat adaptation. Heredity 125 (6), 417–430.

Iizumi, T., Kim, W., Nishimori, M., 2019. Modeling the global sowing and harvesting windows of major crops around the year 2000. J. Adv. Model. Earth Sy. 11 (1), 99–112.

Jagadish, K.S.V., et al., 2014. Agronomic and physiological responses to high temperature, drought, and elevated CO_2 interactions in cereals. Adv. Agron. 127, 111–156.

Jiang, C.Y., Ryu, Y., Wang, H., Keenan, T.F., 2020. An optimality-based model explains seasonal variation in C_3 plant photosynthetic capacity. Glob. Chang. Biol. 26 (11), 6493–6510.

Karger, D.N., Lange, S., Hari, C., Reyer, C.P., Zimmermann, N.E., 2021. CHELSA-W5E5 v1. 1: W5E5 v1. 0 downscaled with CHELSA v2. 0. ISIMIP Repository. https://doi.org/10.48364/ISIMIP.

Kotsuki, S., Tanaka, K., 2015. SACRA – a method for the estimation of global high-resolution crop calendars from a satellite-sensed NDVI. Hydrol. Earth Syst. Sci. 19 (11), 4441–4461.

Lange, S., Büchner, M., 2022. Secondary ISIMIP3b bias-Adjusted Atmospheric Climate Input Data.

Latiri, K., Lhomme, J.P., Annabi, M., Setter, T.L., 2010. Wheat production in Tunisia: Progress, inter-annual variability and relation to rainfall. Eur. J. Agron. 33 (1), 33–42.

Lesk, C., et al., 2021. Stronger temperature–moisture couplings exacerbate the impact of climate warming on global crop yields. Nat. Food. 2 (9), 683–691.

Lilley, J.M., Flohr, B.M., Whish, J.P.M., Farre, I., Kirkegaard, J.A., 2019. Defining optimal sowing and flowering periods for canola in Australia. Field Crop Res. 235, 118–128.

Liu, Y., et al., 2018. Modelling the impacts of climate change and crop management on phenological trends of spring and winter wheat in China. Agric. For. Meteorol. 248, 518–526.

Lobell, D.B., Sibley, A., Ortiz-Monasterio, J.I., 2012. Extreme heat effects on wheat senescence in India. Nat. Clim. Chang. 2 (3), 186–189.

Lobell, D.B., Ortiz-Monasterio, J.I., Sibley, A.M., Sohu, V.S., 2013. Satellite detection of earlier wheat sowing in India and implications for yield trends. Agric. Syst. 115, 137–143.

Mathison, C., Deva, C., Falloon, P., Challinor, A.J., 2018. Estimating sowing and harvest dates based on the Asian summer monsoon. Earth Syst. Dynam. 9 (2), 563–592.

Meek, D.W., Hatfield, J.L., Howell, T.A., Idso, S.B., Reginato, R.J., 1984. A generalized relationship between photosynthetically active radiation and solar-radiation. Agron. J. 76 (6), 939–945.

Mengoli, G., et al., 2022. Ecosystem photosynthesis in land-surface models: a first-principles approach incorporating acclimation. J. Adv. Model. Earth Sy. 14 (1), e2021MS002767.

Minoli, S., Egli, D.B., Rolinski, S., Muller, C., 2019. Modelling cropping periods of grain crops at the global scale. Glob. Planet. Chang. 174, 35–46.

Mueller, N.D., et al., 2012. Closing yield gaps through nutrient and water management. Nature 490 (7419), 254–257.

Mueller, B., et al., 2015. Lengthening of the growing season in wheat and maize producing regions. Weather Clim. Extremes 9, 47–56.

Olesen, J.E., et al., 2012. Changes in time of sowing, flowering and maturity of cereals in Europe under climate change. Food Addit. Contam. Part A Chem. Anal. Control Expo. Risk Assess 29 (10), 1527–1542.

Ortiz-Bobea, A., Ault, T.R., Carrillo, C.M., Chambers, R.G., Lobel, D.B., 2021. Anthropogenic climate change has slowed global agricultural productivity growth. Nat. Clim. Chang. 11 (4), 306–U28.

Perry, E.D., Yu, J., Tack, J., 2020. Using insurance data to quantify the multidimensional impacts of warming temperatures on yield risk. Nat. Commun. 11 (1), 4542.

Portmann, F.T., Siebert, S., Doll, P., 2010. MIRCA2000-global monthly irrigated and rainfed crop areas around the year 2000: a new high-resolution data set for agricultural and hydrological modeling. Global Biogeochem. Cy. 24, GB1011.

Pörtner, H.O., et al., 2022. Climate Change 2022: Impacts, Adaptation and Vulnerability. IPCC.

Prentice, I.C., Dong, N., Gleason, S.M., Maire, V., Wright, I.J., 2014. Balancing the costs of carbon gain and water transport: testing a new theoretical framework for plant functional ecology. Ecol. Lett. 17 (1), 82–91.

Qiao, S.C., Wang, H., Prentice, I.C., Harrison, S.P., 2020. Extending a first-principles primary production model to predict wheat yields. Agric. For. Meteorol. 287, 107932.

Qiao, S.C., Wang, H., Prentice, I.C., Harrison, S.P., 2021. Optimality-based modelling of climate impacts on global potential wheat yield. Environ. Res. Lett. 16 (11), 114013.

Ray, D.K., Ramankutty, N., Mueller, N.D., West, P.C., Foley, J.A., 2012. Recent patterns of crop yield growth and stagnation. Nat. Commun. 3, 1293.

Ren, S., Qin, Q., Ren, H., 2019. Contrasting wheat phenological responses to climate change in global scale. Sci. Total Environ. 665, 620–631.

Rosenzweig, C., et al., 2014. Assessing agricultural risks of climate change in the 21st century in a global gridded crop model intercomparison. Proc. Natl. Acad. Sci. U. S. A. 111 (9), 3268–3273.

Sacks, W.J., Deryng, D., Foley, J.A., Ramankutty, N., 2010. Crop planting dates: an analysis of global patterns. Glob. Ecol. Biogeogr. 19 (5), 607–620.

Sandhu, S.S., Kaur, P., Gill, K.K., Vashisth, B.B., 2020. The effect of recent climate shifts on optimal sowing windows for wheat in Punjab, India. J. Water Clim. Change 11 (4), 1177–1190.

Schaphoff, S., et al., 2018. LPJmL4-a dynamic global vegetation model with managed land - part 1: model description. Geosci. Model Dev. 11 (4), 1343–1375.

Schlenker, W., Roberts, M.J., 2009. Nonlinear temperature effects indicate severe damages to U.S. crop yields under climate change. Proc. Natl. Acad. Sci. U. S. A. 106 (37), 15594–15598.

Sheehan, H., Bentley, A., 2021. Changing times: opportunities for altering winter wheat phenology. Plants People Planet 3 (2), 113–123.

Sperber, K., et al., 2013. The Asian summer monsoon: an intercomparison of CMIP5 vs. CMIP3 simulations of the late 20th century. Clim. Dyn. 41 (9–10), 2711–2744.

Stehfest, E., Heistermann, M., Priess, J.A., Ojima, D.S., Alcamo, J., 2007. Simulation of global crop production with the ecosystem model DayCent. Ecol. Model. 209 (2–4), 203–219.

Stephens, D.J., Lyons, T.J., 1998. Variability and trends in sowing dates across the Australian wheatbelt. Aust. J. Agric. Res. 49 (7).

Stocker, B.D., et al., 2020. P-model v1.0: an optimality -based light use efficiency model for simulating ecosystem gross primary production. Geosci. Model Dev. 13 (3), 1545–1581.

Tack, J., Barkley, A., Nalley, L.L., 2015. Effect of warming temperatures on US wheat yields. Proc. Natl. Acad. Sci. U. S. A. 112 (22), 6931–6936.

Tan, S., Wang, H., Prentice, I.C., Yang, K., 2021. Land-surface evapotranspiration derived from a first-principles primary production model. Environ. Res. Lett. 16 (10), 104047.

Templ, B., et al., 2018. Pan European Phenological database (PEP725): a single point of access for European data. Int. J. Biometeorol. 62 (6), 1109–1113.

Trevaskis, B., 2010. The central role of the VERNALIZATION1 gene in the VERNALIZATION response of cereals. Funct. Plant Biol. 37 (6), 479–487.

van Bussel, L.G.J., Stehfest, E., Siebert, S., Müller, C., Ewert, F., 2015. Simulation of the phenological development of wheat and maize at the global scale. Glob. Ecol. Biogeogr. 24 (9), 1018–1029.

Villegas, D., et al., 2016. Daylength, temperature and solar radiation effects on the phenology and yield formation of spring durum wheat. J. Agron. Crop Sci. 202 (3), 203–216.

Waha, K., van Bussel, L.G.J., Muller, C., Bondeau, A., 2012. Climate-driven simulation of global crop sowing dates. Glob. Ecol. Biogeogr. 21 (2), 247–259.

Wang, E., et al., 2017a. The uncertainty of crop yield projections is reduced by improved temperature response functions. Nat. Plants 3, 17102.

Wang, H., et al., 2017b. Towards a universal model for carbon dioxide uptake by plants. Nat. Plants 3 (9), 734–741.

Wang, X.H., et al., 2020. Emergent constraint on crop yield response to warmer temperature from field experiments. Nat. Sustain. 3 (11), 908–916.

Wang, C., et al., 2022. Occurrence of crop pests and diseases has largely increased in China since 1970. Nat. Food. 3 (1), 57–65.

Zhang, H.P., et al., 2016. Relative yield and profit of Australian hybrid compared with open-pollinated canola is largely determined by growing-season rainfall. Crop. Pasture. Sci. 67 (3–4), 323–331.

Zhao, C., et al., 2016. Field warming experiments shed light on the wheat yield response to temperature in China. Nat. Commun. 7 (1), 13530.

Zhao, C., et al., 2017. Temperature increase reduces global yields of major crops in four independent estimates. Proc. Natl. Acad. Sci. U. S. A. 114 (35), 9326–9331.